ANALYTICAL APPROACH TO 2.5D SOUND FIELD CONTROL USING A CIRCULAR DOUBLE-LAYER ARRAY OF FIXED-DIRECTIVITY LOUDSPEAKERS

Takuma Okamoto

National Institute of Information and Communications Technology
3-5, Hikaridai, Seika-cho, Soraku-gun, Kyoto, 619-0289, Japan
okamoto@nict.go.jp

ABSTRACT

This paper provides a regularization-free analytical approach to 2.5D interior and exterior sound field control using a circular double-layer array of fixed-directivity loudspeakers not only to provide a desired sound field inside the array but also to reduce the sound energy outside of it in the horizontal plane. The proposed method analytically derives the driving functions of the inner and outer circular arrays based on 2.5D spherical harmonic expansion to simultaneously control both sound fields inside and outside the array by a mode-matching framework. The results of computer simulations show that the proposed method is certainly effective compared with the conventional least squares approach that requires regularization schemes in terms of synthesis accuracy inside the listening zone over a wideband frequency range and the acoustic contrast between the quiet zone and the synthesis center at low frequencies.

Index Terms— Interior and exterior sound field control, circular loudspeaker array, fixed-directivity loudspeaker, 2.5D sound field synthesis, Ambisonics

1. INTRODUCTION

In typical sound field synthesis approaches, such as wave field synthesis [1, 2] and higher-order Ambisonics (HOA) [3–5], only the desired synthesis region is considered [6], and undesired sound pressures are radiated to other regions. In applying sound field synthesis in actual environments, it is crucial not only to provide a sound field at a desired region but also to reduce the sound energy in other regions.

Multizone sound field synthesis approaches have been investigated to simultaneously control multiple sound fields in multiple regions [7–14]. In these approaches, however, undesired regions remain.

To synthesize a desired sound field inside a loudspeaker array and completely reduce the undesired sound energy outside of it, 2D interior and exterior sound field control approaches with circular arrays of first-order [15] and higher-order [16] line sources have been proposed. An analytical driving function of a circular first-order line source has been derived [15], based on the Kirchhoff-Helmholtz integral [17] and the Fourier series expansion [17].

For actual implementations, sound field synthesis systems are frequently simplified for synthesis in the horizontal plane. The sound sources are then arranged on a line or a circle. In actual implementations, 3D monopole sources (instead of 2D line sources) are usually

employed for the sound sources. Such approaches are called 2.5D sound field synthesis [5, 18–21].

Since implementing line sources, especially first- and higher-order line sources, is difficult in actual 3D environments, a 2.5D interior and exterior sound field control approach in the horizontal plane using a circular double-layer array of fixed-directivity loudspeakers [22] has been proposed [23] and investigated [24–26]. Experimental validation with an actually implemented array has also been presented [27]. This method is based on the least squares (LS) solution, which is numerically calculated using control points and loudspeaker positions. However, the LS-based approach is quite unstable because the acoustic inverse problem is very ill-conditioned [17]. To stably calculate the well-conditioned inversion and driving signals, regularization schemes are required, such as the truncated singular value decomposition (SVD) method or Tikhonov regularization [28]. In the LS method, repeated calculations of the inversion and driving signals are needed to select the optimal regularization parameters [29].

To avoid the regularization problem in the conventional LS method, this paper provides a regularization-free analytical approach to 2.5D interior and exterior sound field control using a circular double-layer array of fixed-directivity loudspeakers. The interior and exterior sound fields produced by the circular double-layer array of fixed-directivity loudspeakers are represented as 2.5D spherical harmonic expansion and the driving functions of the inner and outer arrays are analytically derived by extending 2.5D HOA [5, 18–21].

2. FOURIER SERIES AND SPHERICAL HARMONIC EXPANSIONS OF SOUND FIELDS

In this section, we briefly introduce the Fourier series expansion of a 2D sound field and the spherical harmonic expansion of a 3D sound field produced by a fixed-directivity loudspeaker.

2.1. Fourier series expansion of 2D sound fields

Spherical coordinates relative to Cartesian coordinates are defined in Fig. 1.

The interior expansion of a 2D sound field ($\theta = \pi/2$) in a region that is homogeneous and free of sources is given as

$$S(r, \phi) = \sum_{m=-\infty}^{\infty} \mathring{A}_m J_m(kr) e^{jm\phi}, \qquad (1)$$

where $\mathring{A}_m$ and J_m are the interior sound field expansion coefficients and the m-th order Bessel function, k is the wavenumber [17], and
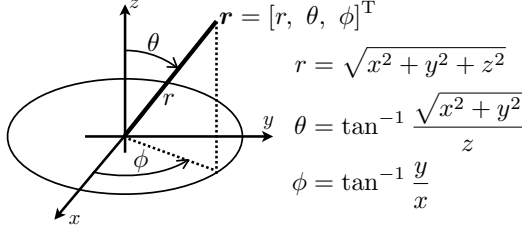
Fig. 1. Definition of spherical coordinates relative to Cartesian coordinates.

$j = \sqrt{-1}$. The corresponding expansion for regions exterior to any sound sources is given as

$$S(r, \phi) = \sum_{m=-\infty}^{\infty} \mathring{B}_m H_m(kr) e^{jm\phi}, \qquad (2)$$

where $\mathring{B}_m$ and H_m are the exterior sound field expansion coefficients and the m-th order Hankel function of the first kind [17].

2.2. Spherical harmonic expansion of 3D sound field produced by a fixed-directivity loudspeaker

As in previous research [22], the sound pressure at $\boldsymbol{r}$, produced by a fixed-directivity loudspeaker located at $\boldsymbol{r}_0$, is modeled as

$$S(\boldsymbol{r}, \boldsymbol{r}_0) = \frac{e^{jk|\boldsymbol{r}-\boldsymbol{r}_0|}}{4\pi|\boldsymbol{r}-\boldsymbol{r}_0|} \left\{ a - (1-a) \left[1 + \frac{j}{k|\boldsymbol{r}-\boldsymbol{r}_0|} \right] \cos\alpha \right\}, \qquad (3)$$

where a is the first-order weighting parameter and α is the angle from the loudspeaker axis.

When the main lobe of $S(\boldsymbol{r}, \boldsymbol{r}_0)$ points toward the origin, the spherical harmonic expansions of (3) for $r < r_0$ and $r > r_0$ are given as

$$S(\boldsymbol{r}, \boldsymbol{r}_0) = jk \sum_{n=0}^{\infty} \sum_{m=-n}^{n} j_n(kr) \{ah_n(kr_0)$$
$$-j(1-a)h_n'(kr_0)\} Y_n^m(\theta, \phi) Y_n^m(\theta_0, \phi_0)^*, \qquad r < r_0, \quad (4)$$

$$S(\boldsymbol{r}, \boldsymbol{r}_0) = jk \sum_{n=0}^{\infty} \sum_{m=-n}^{n} h_n(kr) \{aj_n(kr_0)$$
$$-j(1-a)j_n'(kr_0)\} Y_n^m(\theta, \phi) Y_n^m(\theta_0, \phi_0)^*, \qquad r > r_0, \quad (5)$$

where j_n and j_n' are the n-th order spherical Bessel function and its derivative, h_n and h_n' are the n-th order spherical Hankel function of the first kind and its derivative, and Y_n^m is the m-th order spherical harmonics of the n-th degree [17].

3. ANALYTICAL DRIVING FUNCTION OF A CIRCULAR DOUBLE-LAYER SOUND SOURCE

In the proposed approach, we first consider a continuous circular double-layer sound source distribution with radii r_1 and r_2 ($r_1 < r_2$) centered at the origin on the x-y plane instead of a circular double-layer loudspeaker array (Fig. 2). A sound field synthesized by a continuous circular double-layer sound source is given as

$$S(r, \theta, \phi) = \int_0^{2\pi} D_1(\phi_0) T_1(\boldsymbol{r}, \boldsymbol{r}_1) + D_2(\phi_0) T_2(\boldsymbol{r}, \boldsymbol{r}_2) d\phi_0, \quad (6)$$
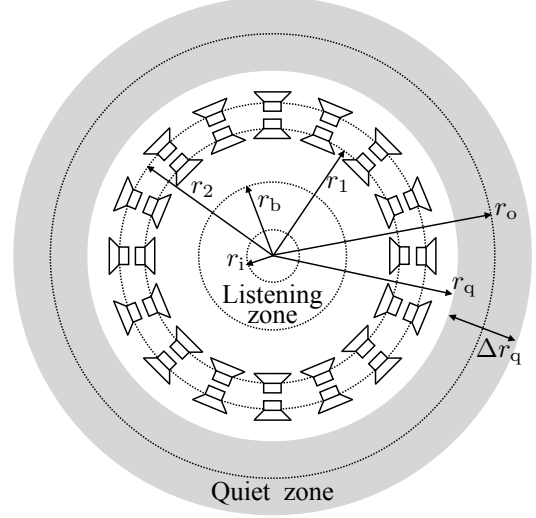

Fig. 2. Arrangements of circular double-layer array of fixed-directivity loudspeakers and listening and quiet zones.

where $D_1(\phi_0)$ and $D_2(\phi_0)$ are the driving functions of the inner and outer circular sources and $T_1(\boldsymbol{r}, \boldsymbol{r}_1)$ and $T_2(\boldsymbol{r}, \boldsymbol{r}_2)$ are the transfer functions from sound source positions $\boldsymbol{r}_1 = [r_1, \pi/2, \phi_0]$ and $\boldsymbol{r}_2 = [r_2, \pi/2, \phi_0]$ to receiver position $\boldsymbol{r}$. Similar to a previous work [23], these transfer functions are modeled as a weighted combination of a monopole and a dipole with the main lobes of $T_1(\boldsymbol{r}, \boldsymbol{r}_1)$ and $T_2(\boldsymbol{r}, \boldsymbol{r}_2)$ pointing toward and away from the center, respectively. Under the free-field assumption, $T_1(\boldsymbol{r}, \boldsymbol{r}_1)$ and $T_2(\boldsymbol{r}, \boldsymbol{r}_2)$ are described as

$$T_1(\boldsymbol{r}, \boldsymbol{r}_1) = \frac{e^{jk|\boldsymbol{r}-\boldsymbol{r}_1|}}{4\pi|\boldsymbol{r}-\boldsymbol{r}_1|} \left\{ a - (1-a) \left[1 + \frac{j}{k|\boldsymbol{r}-\boldsymbol{r}_1|} \right] \cos\alpha \right\}, \qquad (7)$$

$$T_2(\boldsymbol{r}, \boldsymbol{r}_2) = \frac{e^{jk|\boldsymbol{r}-\boldsymbol{r}_2|}}{4\pi|\boldsymbol{r}-\boldsymbol{r}_2|} \left\{ a + (1-a) \left[1 + \frac{j}{k|\boldsymbol{r}-\boldsymbol{r}_2|} \right] \cos\alpha \right\}. \qquad (8)$$

As in [5], when the spatial Fourier series expansion is applied to (6) with $\theta = \pi/2$, the circular convolution theorem holds and (6) is represented as

$$\mathring{S}_m(r) = 2\pi \left\{ \mathring{D}_{m,1} \mathring{T}_{m,1}(r, r_1) + \mathring{D}_{m,2} \mathring{T}_{m,2}(r, r_2) \right\}. \quad (9)$$

Similar to 2.5D HOA [5, 18, 20, 21], the 2.5D spherical harmonic expansions of transfer functions $T_1(\boldsymbol{r}, \boldsymbol{r}_1)$ and $T_2(\boldsymbol{r}, \boldsymbol{r}_2)$ are derived from (4) and (5) and given as

$$\mathring{T}_{m,1}(r_<, r_1) = jk \sum_{n=|m|}^{\infty} j_n(kr) h_{n,1}(a, r_1) Q_n^m P_n^{|m|}(0)^2, \quad (10)$$

$$\mathring{T}_{m,2}(r_<, r_2) = jk \sum_{n=|m|}^{\infty} j_n(kr) h_{n,2}(a, r_2) Q_n^m P_n^{|m|}(0)^2, \quad (11)$$

$$\mathring{T}_{m,1}(r_>, r_1) = jk \sum_{n=|m|}^{\infty} h_n(kr) j_{n,1}(a, r_1) Q_n^m P_n^{|m|}(0)^2, \quad (12)$$

$$\mathring{T}_{m,2}(r_>, r_2) = jk \sum_{n=|m|}^{\infty} h_n(kr) j_{n,2}(a, r_2) Q_n^m P_n^{|m|}(0)^2, \quad (13)$$

where $P_n^{|m|}$ is the $|m|$-th order associated Legendre polynomial of the n-th degree [30] and

$$h_{n,1}(a, r_1) = ah_n(kr_1) - j(1-a)h_n'(kr_1), \qquad (14)$$

$$h_{n,2}(a, r_2) = ah_n(kr_2) + j(1-a)h_n'(kr_2), \qquad (15)$$

$$j_{n,1}(a, r_1) = aj_n(kr_1) - j(1-a)j_n'(kr_1), \qquad (16)$$

$$j_{n,2}(a, r_2) = aj_n(kr_2) + j(1-a)j_n'(kr_2), \qquad (17)$$

$$Q_n^m = \frac{2n+1}{4\pi} \frac{(n-|m|)!}{(n+|m|)!}. \qquad (18)$$

Even though r is completely canceled in the driving functions in the 2D and 3D cases, the driving function of 2.5D HOA depends on r and accurate sound pressures are synthesized at the reference circle [5, 18–21].

In the proposed approach, to simultaneously control the sound fields both inside and outside the circular source, the reference distances for the listening and quiet zones inside and outside of it are set to r_i ($0 < r_i < r_1$) and r_o ($r_o > r_2$), respectively. From (1) and (2), the sound pressures inside and outside the circular source are then set to

$$\mathring{S}_m(r_i) = \mathring{A}_m J_m(kr_i), \qquad (19)$$

$$\mathring{S}_m(r_o) = \mathring{B}_m H_m(kr_o) = 0. \qquad (20)$$

(19) and (20) are substituted into (9) and represented in matrix form:

$$2\pi \begin{bmatrix} \mathring{T}_{m,1}(r_{i<}, r_1) & \mathring{T}_{m,2}(r_{i<}, r_2) \\ \mathring{T}_{m,1}(r_{o>}, r_1) & \mathring{T}_{m,2}(r_{o>}, r_2) \end{bmatrix} \begin{bmatrix} \mathring{D}_{m,1} \\ \mathring{D}_{m,2} \end{bmatrix}$$
$$= \begin{bmatrix} \mathring{A}_m J_m(kr_i) \\ 0 \end{bmatrix}. \qquad (21)$$

Then driving functions $\mathring{D}_{m,1}$ and $\mathring{D}_{m,2}$ are directly derived as

$$\mathring{D}_{m,1} = \frac{\mathring{T}_{m,2}(r_{o>}, r_2)\mathring{A}_m J_m(kr_i)}{2\pi \mathring{T}_m(r_1, r_2, r_i, r_o)}, \qquad (22)$$

$$\mathring{D}_{m,2} = -\frac{\mathring{T}_{m,1}(r_{o>}, r_1)\mathring{A}_m J_m(kr_i)}{2\pi \mathring{T}_m(r_1, r_2, r_i, r_o)}, \qquad (23)$$

where

$$\mathring{T}_m(r_1, r_2, r_i, r_o)$$
$$= \mathring{T}_{m,1}(r_{i<}, r_1)\mathring{T}_{m,2}(r_{o>}, r_2) - \mathring{T}_{m,2}(r_{i<}, r_2)\mathring{T}_{m,1}(r_{o>}, r_1). \qquad (24)$$

The driving function of 2.5D HOA with reference distance $r_{\text{ref}} = 0$ is derived [18] and can synthesize a more accurate sound field than with $r_{\text{ref}} > 0$. To extend the driving functions of the proposed method into those with $r_i = 0$, L'Hôpital's rule [31] and the following approximations for small arguments, i.e., $kr \to 0$ [17],

$$j_n(kr) \approx \frac{(kr)^n}{(2n+1)!!}, \quad \text{and} \quad J_m(kr) \approx \frac{\text{sgn}(m)^{|m|}(kr)^{|m|}}{2^{|m|}|m|!},$$

are also applied in (22) and (23). The driving functions with $r_i = 0$ are then obtained as

$$\mathring{D}_{m,1}\Big|_{r_i=0} = \frac{\mathring{T}_{m,2}(r_{o>}, r_2)\mathring{A}_m C_m}{2\pi j k Q_{|m|}^m P_{|m|}^{|m|}(0)^2 U_m(a, r_1, r_2, r_o)}, \qquad (25)$$

$$\mathring{D}_{m,2}\Big|_{r_i=0} = -\frac{\mathring{T}_{m,1}(r_{o>}, r_1)\mathring{A}_m C_m}{2\pi j k Q_{|m|}^m P_{|m|}^{|m|}(0)^2 U_m(a, r_1, r_2, r_o)}, \qquad (26)$$

where

$$C_m = \frac{\text{sgn}(m)^{|m|}(2|m|+1)!!}{2^{|m|}|m|!}, \qquad (27)$$

$$U_m(a, r_1, r_2, r_o) =$$
$$h_{|m|,1}(a, r_1)\mathring{T}_{m,2}(r_{o>}, r_2) - h_{|m|,2}(a, r_2)\mathring{T}_{m,1}(r_{o>}, r_1), \qquad (28)$$

and sgn in (27) is the sign function.

A continuous circular double-layer source is finally discretized into a circular double-layer loudspeaker array. When the number of loudspeakers of each layer is L, order m of the spatial Fourier series in (25) and (26) can be calculated up to $M = \lfloor (L-1)/2 \rfloor$, where $\lfloor \cdot \rfloor$ is the floor function. The driving signal of each loudspeaker at ϕ_l in the temporal frequency domain is obtained as

$$D(\phi_l) = \sum_{m=-M}^{M} \mathring{D}_m\Big|_{r_i=0} e^{jm\phi_l}, \qquad l = 1, 2, \cdots L. \qquad (29)$$

4. COMPUTER SIMULATIONS

Computer simulations compared the proposed approach with the conventional LS method [23]. In all the simulations, a three-dimensional free field was assumed. The speed of sound c was 343.36 m/s.

As in a previous work [23], the radii of the inner and outer circular arrays of the fixed-directivity loudspeakers, those of the listening and quiet zones were $r_1 = 0.9$ m, $r_2 = 1.0$ m, $r_b = 0.2$ m, and $r_q = 2.0$ m, respectively. The quiet zone width was $\Delta r_q = 1.0$ m. The control distances in the proposed method were set to $r_i = 0$ m and $r_o = 2.5$ m. The arrangement of these radii is depicted in Fig. 2. In the LS method, the listening and quiet zones were sampled at discrete points with 0.05 m spacing between adjacent points. The weighting factor to determine the balance between the potential energy in the quiet zone by the acoustic contrast approach [32] and the mean square error in the listening zone by the pressure matching approach [33] was $\kappa = 0.5$, and truncated SVD regularization [28] and the discrepancy principle with the same parameter in [23] were used to calculate the stable driving signals in the LS method. The total number of loudspeakers was 64 and $L = 32$. The maximum order in (29) was $M = 15$. n in (12), and (13) was truncated to 100. The desired sound field was a plane wave with an amplitude of unity propagating from direction $\Phi = \pi/4$ and $\mathring{A}_m = j^m e^{-jm\Phi}$.

To estimate the synthesized sound field, the synthesis error at position $\boldsymbol{r}$ and the acoustic contrast between position $\boldsymbol{r}$ and the center of the array ($r = 0$) were defined as

$$E(\boldsymbol{r}) = 10 \log_{10} \frac{|S_{\text{des}}(\boldsymbol{r}) - S_{\text{syn}}(\boldsymbol{r})|^2}{|S_{\text{des}}(\boldsymbol{r})|^2}, \qquad (30)$$

$$C(\boldsymbol{r}) = 10 \log_{10} \frac{|S_{\text{syn}}(\boldsymbol{r})|^2}{|S_{\text{syn}}(r = 0)|^2}, \qquad (31)$$

where $S_{\text{des}}(\boldsymbol{r})$ and $S_{\text{syn}}(\boldsymbol{r})$ were the desired and synthesized sound pressures at position $\boldsymbol{r}$, respectively.

Figure 3 shows the results of the synthesized sound field, the previously defined synthesis error (30), and the previously defined acoustic contrast (31) for both the conventional LS and proposed methods using 64 cardioid directivity loudspeakers ($a = 0.5$) at a temporal frequency of $f = 400$ Hz. These results indicate that the proposed approach effectively controlled both the interior and exterior sound fields as well as the conventional LS method.
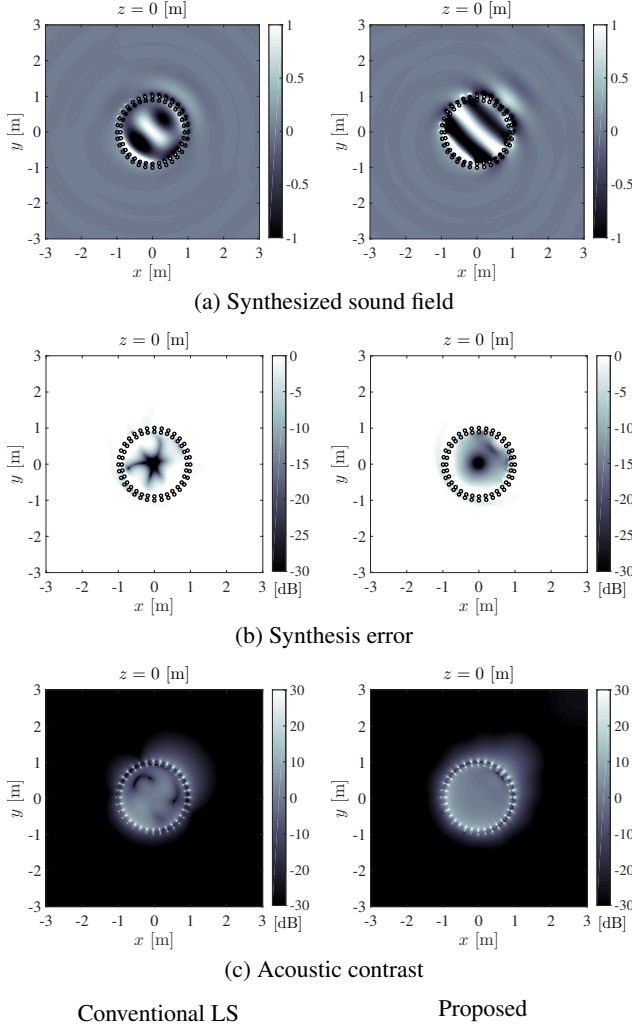
(a) Synthesized sound field

(b) Synthesis error

(c) Acoustic contrast

Conventional LS   Proposed

Fig. 3. Results: (a) synthesized sound field, (b) synthesis error defined in (30), and (c) acoustic contrast defined in (31) for conventional LS and proposed methods using 64 cardioid directivity loudspeakers ($a = 0.5$) at temporal frequency $f = 400\,\mathrm{Hz}$. Black circles in (a) and (b) are 64 loudspeakers.

In addition, the averaged synthesis error inside the listening zone ($r \leq r_\mathrm{b}$) and the acoustic contrast between the quiet zone with width Δr_q and the center of the array up to $f = 2\,\mathrm{kHz}$ are plotted in Figs. 4 and 5, respectively.

As shown in Fig. 4, the results of the averaged synthesis error suggest that the proposed approach clearly outperformed the LS method in terms of synthesis accuracy inside the listening zone at all of the temporal frequencies. This is because it is based on mode matching just like HOA and truncated order $M = 15$ is sufficient to control the sound pressures inside the listening zone up to $f = 2\,\mathrm{kHz}$ whose corresponding order is $kr_\mathrm{b} \approx 7.3 < M$.

The results of the averaged acoustic contrast shown in Fig. 5 indicate that the proposed approach efficiently controlled the quiet zone with an averaged acoustic contrast below $-40\,\mathrm{dB}$ up to around $f_{\mathrm{Nyq},2} \approx 819\,\mathrm{Hz}$, which is the spatial Nyquist frequency of the outer array that corresponds to $kr_2 = M$. This limitation is the same as the conventional 2D analytical approach with first-order line
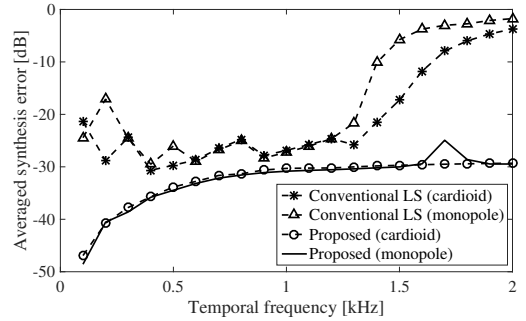

Fig. 4. Results of averaged synthesis error inside listening zone ($r \leq r_\mathrm{b}$) for LS and proposed methods with cardioid directivity ($a = 0.5$) and omni-directional ($a = 1$) loudspeakers.
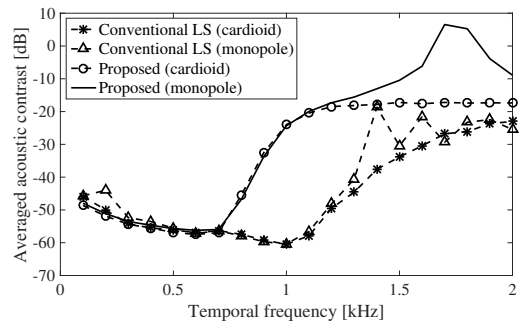

Fig. 5. Results of averaged acoustic contrast between quiet zone and center of array for LS and proposed methods with cardioid directivity ($a = 0.5$) and omni-directional ($a = 1$) loudspeakers.

sources [15]. In the proposed method, the averaged acoustic contrast performance around $f_{\mathrm{Nyq},2}$ was slightly delegated since only the sound pressures on the circle with radius r_o are accurately controlled and the wavelength corresponding to around $f_{\mathrm{Nyq},2}$ was shorter than quiet zone width Δr_q.

As previously examined [23], the results in Figs. 4 and 5 with omni-directional loudspeakers ($a = 1$) are also almost the same as those with cardioid directivity loudspeakers below about 1.2 kHz.

Consequently, the proposed approach based on an analytical solution without regularization is certainly effective compared with the conventional LS method that requires regularization schemes in terms of synthesis accuracy inside the listening zone over a wideband frequency range and the acoustic contrast between the quiet zone and the synthesis center at low frequencies.

5. CONCLUSIONS

This paper proposed a regularization-free analytical method to control 2.5D interior and exterior sound fields using a circular double-layer array of fixed-directivity loudspeakers. The driving functions of the inner and outer circular arrays were analytically derived based on the 2.5D spherical harmonic expansion of the sound field produced by fixed-directivity loudspeakers. The results of computer simulations showed that the proposed method is certainly effective compared with the conventional LS method with regularization in terms of synthesis accuracy inside the listening zone over a wideband frequency range and the acoustic contrast between the quiet zone and the synthesis center at low frequencies.

6. REFERENCES

[1] A. J. Berkhout, D. de Vries, and P. Vogel, "Acoustic control by wave field synthesis," *J. Acoust. Soc. Am.*, vol. 93, no. 5, pp. 2764–2778, May 1993.

[2] S. Spors, R. Rabenstein, and J. Ahrens, "The theory of wave field synthesis revisited," in *Proc. 124th Conv. Audio Eng. Soc.*, May 2008.

[3] J. Daniel, "Spatial sound encoding including near field effect: Introducing distance coding filters and a viable, new Ambisonic format," in *Proc. 23rd Int. Conf. Audio Eng. Soc.*, May 2003.

[4] M. A. Poletti, "Three-dimensional surround sound systems based on spherical harmonics," *J. Audio Eng. Soc.*, vol. 53, no. 11, pp. 1004–1025, Nov. 2005.

[5] J. Ahrens and S. Spors, "An analytical approach to sound field reproduction using circular and spherical loudspeaker distributions," *Acta Acust. Acust.*, vol. 94, no. 6, pp. 988–999, Nov. 2008.

[6] F. Schultz and S. Spors, "Comparing approaches to the spherical and planar single layer potentials for interior sound field synthesis," *Acta Acust. Acust.*, vol. 100, no. 5, pp. 900–911, Sept. 2014.

[7] Y. J. Wu and T. D. Abhayapala, "Spatial multizone soundfield reproduction: Theory and design," *IEEE Trans. Audio, Speech, Lang. Process.*, vol. 19, no. 6, pp. 1711–1720, Aug. 2011.

[8] N. Radmanesh and I. S. Burnett, "Generation of isolated wideband sound fields using a combined two-stage Lasso-LS algorithm," *IEEE Trans. Audio, Speech, Lang. Process.*, vol. 21, no. 2, pp. 378–387, Feb. 2013.

[9] M. A. Poletti and F. M. Fazi, "An approach to generating two zones of silence with application to personal sound systems," *J. Acoust. Soc. Am.*, vol. 137, no. 2, pp. 598–605, Feb. 2015.

[10] T. Betlehem, W. Zhang, M. Poletti, and T. Abhayapala, "Personal sound zones: Delivering interface-free audio to multiple listeners," *IEEE Signal Process. Mag.*, vol. 32, no. 2, pp. 81–91, Mar. 2015.

[11] W. Jin and W. B. Kleijn, "Theory and design of multizone soundfield reproduction using sparse methods," *IEEE/ACM Trans. Audio, Speech, Lang. Process.*, vol. 23, no. 12, pp. 2343–2355, Dec. 2015.

[12] N. Radmanesh, I. S. Burnett, and B. D. Rao, "A Lasso-LS optimization with a frequency variable dictionary in a multizone sound system," *IEEE/ACM Trans. Audio, Speech, Lang. Process.*, vol. 24, no. 3, pp. 583–593, Mar. 2016.

[13] M. A. Poletti and F. M. Fazi, "Generation of half-space sound fields with application to personal sound systems," *J. Acoust. Soc. Am.*, vol. 139, no. 3, pp. 1294–1302, Mar. 2016.

[14] W. Zhang, T. D. Abhayapala, T. Betlehem, and F. M. Fazi, "Analysis and control of multi-zone sound field reproduction using modal-domain approach," *J. Acoust. Soc. Am.*, vol. 140, no. 3, pp. 2134–2144, Sept. 2016.

[15] M. A. Poletti and T. D. Abhayapala, "Interior and exterior sound field control using general two-dimensional first-order sources," *J. Acoust. Soc. Am.*, vol. 129, no. 1, pp. 234–244, Jan. 2011.

[16] M. A. Poletti, T. D. Abhayapala, and P. Samarasinghe, "Interior and exterior sound field control using two dimensional higher-order variable-directivity sources," *J. Acoust. Soc. Am.*, vol. 131, no. 5, pp. 3814–3823, May 2012.

[17] E. G. Williams, *Fourier Acoustics: Sound Radiation and Nearfield Acoustic Holography*, Academic Press, London, UK, 1999.

[18] W. Zhang and T. D. Abhayapala, "2.5D sound field reproduction in higher order Ambisonics," in *Proc. IWAENC*, Sept. 2014, pp. 342–346.

[19] T. Okamoto, "Analytical methods of generating multiple sound zones for open and baffled circular loudspeaker arrays," in *Proc. WASPAA*, Oct. 2015.

[20] T. Okamoto, "2.5D higher-order Ambisonics for a sound field described by angular spectrum coefficients," in *Proc. ICASSP*, Mar. 2016, pp. 326–330.

[21] F. Winter, J. Ahrens, and S. Spors, "On analytic methods for 2.5-D local sound field synthesis using circular distributions of secondary sources," *IEEE/ACM Trans. Audio, Speech, Lang. Process.*, vol. 24, no. 5, pp. 914–926, May 2016.

[22] M. A. Poletti, F. M. Fazi, and P. A. Nelson, "Sound-field reproduction systems using fixed-directivity loudspeakers," *J. Acoust. Soc. Am.*, vol. 127, no. 6, pp. 3590–3601, June 2010.

[23] J.-H. Chang and F. Jacobsen, "Sound field control with a circular double-layer array of loudspeaker," *J. Acoust. Soc. Am.*, vol. 131, no. 6, pp. 4518–4525, June 2012.

[24] J.-H. Chang and F. Jacobsen, "The effect of scattering on sound field control with a circular double-layer array of loudspeakers," in *Proc. 132nd Conv. Audio Eng. Soc.*, Apr. 2012.

[25] J.-H. Chang, F. Agerkvist, and M. Olsen, "Arrangements of a pair of loudspeakers for sound field control with double-layer arrays," in *Proc. 52nd Int. Conf. Audio Eng. Soc.*, Sept. 2013.

[26] Z. Tu, J. Lu, and K. Chen, "Evaluation of robustness of sound field control with a circular double-layer array of loudspeakers," in *Proc. ICSV21*, July 2014.

[27] J.-H. Chang and F. Jacobsen, "Experimental validation of sound field control with a circular double-layer array of loudspeakers," *J. Acoust. Soc. Am.*, vol. 133, no. 4, pp. 2046–2054, Apr. 2013.

[28] P. C. Hansen, *Rank Deficient and Discrete Ill-posed Problems: Numerical Aspects of Linear Inversion*, SIAM, Philadelphia, 1998.

[29] T. Okamoto, S. Enomoto, and R. Nishimura, "Least squares approach in wavenumber domain for sound field recording and reproduction using multiple parallel linear arrays," *Appl. Acoust.*, vol. 86, pp. 95–103, Dec. 2014.

[30] D. Colton and R. Kress, *Inverse Acoustic and Electromagnetic Scattering Theory*, Springer, Berlin, 1998.

[31] M. Abramowitz and I. A. Stegun, *Handbook of Mathematical Functions: with Formulas, Graphs, and Mathematical Tables*, Dover Publications, New York, 1965.

[32] J.-W. Choi and Y.-H. Kim, "Generation of an acoustically bright zone with an illuminated region using multiple sources," *J. Acoust. Soc. Am.*, vol. 111, no. 4, pp. 1695–1700, Apr. 2002.

[33] O. Kirkeby and P. Nelson, "Reproduction of plane wave sound fields," *J. Acoust. Soc. Am.*, vol. 94, no. 5, pp. 2992–3000, Nov. 1993.